

^{40}K ^{87}Rb Feshbach Resonances: Modeling the interatomic potential

C. Klempt, T. Henninger, O. Topic, J. Will, W. Ertmer, E. Tiemann and J. Arlt
Institut für Quantenoptik, Leibniz Universität Hannover, Welfengarten 1, D-30167 Hannover, Germany
(Dated: October 31, 2018)

We have observed 28 heteronuclear Feshbach resonances in 10 spin combinations of the hyperfine ground states of a ^{40}K ^{87}Rb mixture. The measurements were performed by observing the loss rates from an atomic mixture at magnetic fields between 0 and 700 G. This data was used to significantly refine an interatomic potential derived from molecular spectroscopy, yielding a highly consistent model of the ^{40}K ^{87}Rb interaction. Thus, the measured resonances can be assigned to the corresponding molecular states. In addition, this potential allows for an accurate calculation of the energy differences between highly excited levels and the rovibrational ground level. This information is of particular relevance for the formation of deeply bound heteronuclear molecules. Finally, the model is used to predict Feshbach resonances in mixtures of ^{87}Rb combined with ^{39}K or ^{41}K .

One of the current challenges in modern atomic and molecular physics is the production of quantum degenerate, dilute ensembles with dipolar interaction. Especially for the case of ultracold dipolar fermions, a large variety of interesting phenomena has been predicted, including superfluid pairing [1, 2], quantum computing [3, 4] and the fractional quantum Hall effect [5]. Recently, first evidence of dipolar interactions in bosonic chromium atoms has been reported [6]. However, most of the predicted effects will be difficult to observe in atomic systems, since the dipolar interaction is typically dominated by the contact interaction. A fascinating alternative is the preparation of quantum degenerate samples of molecules in their absolute ground state [7]. One obvious approach is direct cooling of molecules ([8, 9] and references therein). Alternatively, weakly bound Feshbach molecules [10, 11, 12, 13, 14, 15, 16] can be created from degenerate atomic ensembles. Subsequently a second process, such as Stimulated Raman Adiabatic Passage [17], can be used to form tightly bound molecules [18, 19, 20, 21]. The mixture of ^{40}K and ^{87}Rb is a promising candidate for the production of polar molecules, since the first heteronuclear Feshbach molecules were recently obtained in this mixture [16] and pathways to deeply bound molecules are under investigation [22]. The precise understanding of the interatomic potential presented in this letter is of vital importance for the development of such paths towards deeply bound molecules.

In our experiments, 20 previously unknown s-wave Feshbach resonances in stable spin configurations of ^{40}K and ^{87}Rb were detected and identified using the following procedure. An initial prediction of the resonances was based on precise potentials of the $X^1\Sigma^+$ and $a^3\Sigma^+$ states obtained from molecular spectroscopy [23]. The asymptotic parts of these potentials were then adjusted to reproduce the 8 previously known resonances [24, 25, 26, 27]. Our measurement of a total of 28 resonance positions as described below allowed for a significant refinement of the potential. This technique

provides a potential which is precise both at small and large internuclear separation. Thus, it allows for the calculation of the energy difference between the Feshbach molecules and deeply bound molecules in the ground states. This difference is the key parameter for the production of deeply bound quantum degenerate molecules with large dipole moments.

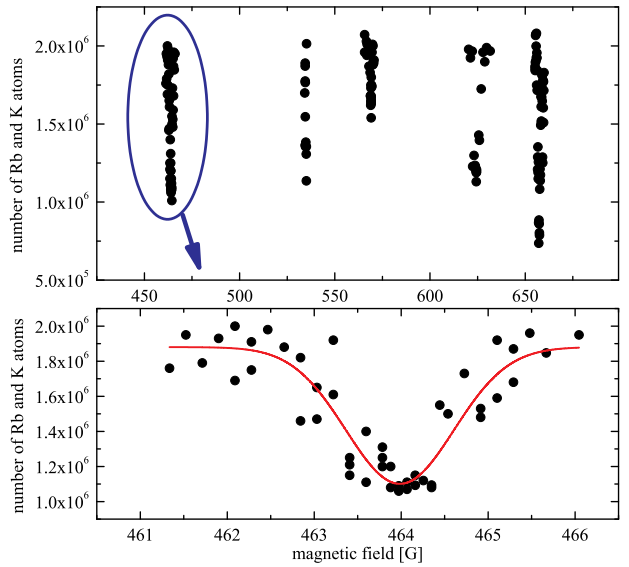


FIG. 1: Total atom number as a function of the magnetic field in the ^{87}Rb $|1, 1\rangle$, ^{40}K $|9/2, -5/2\rangle$ state.

The following experimental procedure was used to detect heteronuclear Feshbach resonances in a ^{40}K ^{87}Rb mixture. A two-species magneto-optical trap (MOT) was loaded with 5×10^9 ^{87}Rb atoms and 2×10^8 ^{40}K atoms using light-induced atom desorption at 395 nm. This process provides an efficient, switchable source of atoms [28]. The desorption light was switched off before the end of the MOT phase in order to benefit from a better vacuum. Both species were cooled in an optical molasses and optically pumped to the fully

stretched low-field seeking Zeeman states, $|f, m_f\rangle = |2, 2\rangle$ for ^{87}Rb and $|9/2, 9/2\rangle$ for ^{40}K . The atoms were subsequently loaded into a magnetic quadrupole trap and mechanically transported to an ultra-high vacuum cell. There, these atoms were transferred into a harmonic trap in QUIC configuration [29] with ^{87}Rb trap frequencies of $2\pi \times 230$ Hz ($2\pi \times 23$ Hz) in radial (axial) direction. The ^{87}Rb atoms were cooled by forced radio frequency (RF) evaporation and in turn cooled the ^{40}K atoms sympathetically. This evaporation was terminated shortly before reaching quantum degeneracy and an equal mixture of 2×10^6 ^{87}Rb and ^{40}K atoms at a temperature of 1.1 μK with no discernible fraction in other Zeeman states was obtained. This ensemble was transferred into an optical dipole trap formed by a monolithic Nd:YAG laser at a wavelength of 1064 nm with a trap depth of 170 μK and radial (axial) trapping frequencies of $2\pi \times 2$ kHz ($2\pi \times 25$ Hz) for ^{87}Rb . In the dipole trap the mixture had a temperature of 4 μK and a maximum ^{87}Rb density of 2×10^{14} atoms/cm³.

The use of an optical dipole trap allows for the free choice of the magnetic field and thus enables an investigation of Feshbach resonances. To produce strong magnetic fields up to 700 G, the quadrupole coils of the magnetic trap are operated in quasi-Helmholtz configuration. This field was raised to 10 G to transfer the ^{87}Rb atoms from the $|2, 2\rangle$ state to the $|1, 1\rangle$ state by a microwave rapid adiabatic passage. Starting at 6.8561 GHz, the microwave frequency was reduced by 800 kHz within a 50 ms interval. The transfer efficiency was better than 90% and the remaining atoms in the $|2, 2\rangle$ state were removed with a resonant light pulse. Afterwards, the magnetic field was raised to 19 G to allow for a transfer of the ^{40}K atoms to a specific spin state. To access the nine $|f = 9/2, m_f = -9/2 \dots 7/2\rangle$ states, radio frequency sweeps with a speed of 10 kHz/ms starting at 6.56 MHz were used. The desired spin state was selected by adjusting the end of the RF sweep.

If needed, the magnetic field was raised to 29 G to transfer the ^{87}Rb atoms to the $|1, 0\rangle$ or $|1, -1\rangle$ state by using RF sweeps. The final mixture is stable against spin changing collisions as long as one of the components is in the lowest energy spin state. In this case, the spin exchange is either forbidden by energy or by angular momentum conservation, since the ^{87}Rb Zeeman structure is inverted. This allows for the investigation of Feshbach resonances in a total of 12 different spin configurations, nine of which have not been investigated so far [24, 25, 26, 27].

The Feshbach resonances in all of these states were located by detecting inelastic losses. After preparing the spin mixture of interest, the magnetic field was quickly increased to a certain value. The atoms were held at this magnetic field for a time between 0.5 s and 2 s. The hold time was chosen such that the maximum loss of atoms was approximately 50% . On the one hand, this

TABLE I: Magnetic-field positions and widths of all investigated s-wave Feshbach resonances in the mixture of ^{40}K and ^{87}Rb . Quantum numbers are given for the corresponding molecular levels without magnetic field. The whole multiplet is given for the total angular momentum F , since its splitting is smaller than the Zeeman energy (see Fig. 2) and F is no longer a good quantum number. All molecular states are mixed levels of the last bound vibrational states $v_a = 30$ and $v_x = 98$. Note that the experimental width σ_{exp} does not correspond directly to the theoretical width Δ_{th} (see definition in text).

$m_{\text{Rb}},$ m_{K}	B_{th} (G)	$-\Delta_{\text{th}}$ (G)	B_{exp} (G)	σ_{exp} (G)	F	$f_{\text{Rb}}/$ f_{K}	
$1, \frac{7}{2}$	298.70	0.61	298.67	< 0.12	$\frac{9}{2}, \frac{11}{2}$	$1/\frac{9}{2}$	[25]
$1, \frac{5}{2}$	177.57	< 0.005	—	—	$\frac{7}{2}, \frac{9}{2}, \frac{11}{2}$	$1/\frac{9}{2}$	
	359.86	0.88	359.70	< 0.1	$\frac{7}{2}, \frac{9}{2}, \frac{11}{2}$	$1/\frac{9}{2}$	
$1, \frac{3}{2}$	184.56	< 0.005	—	—	$\frac{7}{2}, \frac{9}{2}, \frac{11}{2}$	$1/\frac{9}{2}$	
	399.12	0.85	399.16	0.61	$\frac{7}{2}, \frac{9}{2}, \frac{11}{2}$	$1/\frac{9}{2}$	
$1, \frac{1}{2}$	190.25	< 0.005	—	—	$\frac{7}{2}, \frac{9}{2}, \frac{11}{2}$	$1/\frac{9}{2}$	
	424.37	0.76	424.39	0.30	$\frac{7}{2}, \frac{9}{2}, \frac{11}{2}$	$1/\frac{9}{2}$	
	660.15	0.11	660.23	0.42	$\frac{3}{2} \dots \frac{11}{2}$	$2/\frac{7}{2}$	
$1, -\frac{1}{2}$	194.90	< 0.005	—	—	$\frac{7}{2}, \frac{9}{2}, \frac{11}{2}$	$1/\frac{9}{2}$	
	441.87	0.66	442.06	0.55	$\frac{7}{2}, \frac{9}{2}, \frac{11}{2}$	$1/\frac{9}{2}$	
	612.69	0.08	612.48	< 0.24	$\frac{3}{2} \dots \frac{11}{2}$	$1/\frac{7}{2}$	
	688.55	0.01	688.56	0.34	$\frac{5}{2}, \frac{7}{2}, \frac{9}{2}$	$2/\frac{7}{2}$	
$1, -\frac{3}{2}$	198.74	< 0.005	—	—	$\frac{7}{2}, \frac{9}{2}, \frac{11}{2}$	$1/\frac{9}{2}$	
	454.66	0.55	454.88	0.82	$\frac{7}{2}, \frac{9}{2}, \frac{11}{2}$	$1/\frac{9}{2}$	
	571.19	0.05	571.17	< 0.24	$\frac{3}{2} \dots \frac{11}{2}$	$2/\frac{7}{2}$	
	623.23	0.02	623.29	0.45	$\frac{5}{2}, \frac{7}{2}, \frac{9}{2}$	$1/\frac{7}{2}$	
	669.87	0.81	669.84	< 0.14	$\frac{3}{2} \dots \frac{11}{2}$	$2/\frac{7}{2}$	
$1, -\frac{5}{2}$	201.96	< 0.005	—	—	$\frac{7}{2}, \frac{9}{2}, \frac{11}{2}$	$1/\frac{9}{2}$	
	464.02	0.42	463.89	0.62	$\frac{7}{2}, \frac{9}{2}, \frac{11}{2}$	$1/\frac{9}{2}$	
	534.66	0.02	534.68	< 0.20	$\frac{3}{2} \dots \frac{11}{2}$	$2/\frac{7}{2}$	
	568.14	0.03	568.28	0.55	$\frac{5}{2}, \frac{7}{2}, \frac{9}{2}$	$1/\frac{7}{2}$	
	624.89	0.75	624.29	1.56	$\frac{3}{2} \dots \frac{11}{2}$	$1/\frac{7}{2}$	
	657.09	2.66	657.24	0.97	$\frac{5}{2}, \frac{7}{2}, \frac{9}{2}$	$2/\frac{7}{2}$	
$1, -\frac{7}{2}$	204.65	< 0.002	—	—	$\frac{7}{2}, \frac{9}{2}, \frac{11}{2}$	$1/\frac{9}{2}$	
	469.48	0.28	469.54	< 0.14	$\frac{7}{2}, \frac{9}{2}, \frac{11}{2}$	$1/\frac{9}{2}$	[25]
	523.04	0.06	523.04	< 0.2	$\frac{5}{2}, \frac{7}{2}, \frac{9}{2}$	$1/\frac{7}{2}$	
	584.58	0.70	584.42	0.35	$\frac{5}{2} \dots \frac{11}{2}$	$1/\frac{7}{2}$	[25]
	598.32	2.55	598.24	0.32	$\frac{5}{2}, \frac{7}{2}, \frac{9}{2}$	$2/\frac{7}{2}$	[25]
	697.56	0.16	697.80	0.49	$\frac{5}{2}, \frac{7}{2}, \frac{9}{2}$	$1/\frac{7}{2}$	[25]
	$1, -\frac{9}{2}$	207.02	< 0.001	—	—	$\frac{7}{2}, \frac{9}{2}, \frac{11}{2}$	$1/\frac{9}{2}$
462.45		0.06	462.41	< 0.20	$\frac{7}{2}, \frac{9}{2}, \frac{11}{2}$	$1/\frac{9}{2}$	
495.71		0.14	495.57	< 0.20	$\frac{7}{2}, \frac{9}{2}$	$1/\frac{7}{2}$	[25, 26, 27]
546.89		3.07	546.71	0.68	$\frac{7}{2}, \frac{9}{2}$	$1/\frac{7}{2}$	[25, 26, 27]
$0, -\frac{9}{2}$	659.68	0.80	659.52	0.39	$\frac{7}{2}, \frac{9}{2}, \frac{11}{2}$	$2/\frac{9}{2}$	[25]
	430.71	0.11	430.93	0.63	$\frac{9}{2}, \frac{11}{2}$	$1/\frac{9}{2}$	
	546.08	3.16	546.13	0.43	$\frac{9}{2}$	$1/\frac{7}{2}$	

ensures a good signal-to-noise ratio, on the other hand, the population of other Zeeman states due to inelastic

collisions remains negligible. After this hold time, the magnetic field was lowered to a small bias field perpendicular to the direction of detection. Both species were detected independently by absorption imaging after ballistic expansion. The spin states were separated in a Stern-Gerlach experiment by a strong magnetic gradient applied for 4 ms during the initial stage of the expansion. This allowed us to verify that no unwanted spin components were populated. The total number of atoms was measured as a function of the applied magnetic field. Figure 1 shows the result of these measurements for the spin configuration ^{87}Rb $|1, 1\rangle$ and ^{40}K $|9/2, -5/2\rangle$. For each resonance, a Gaussian fit was used to extract the center position and the $1/e^2$ -width of the resonance. Due to slight asymmetries of the resonances and shot-to-shot atom number fluctuations of $\sim 10\%$, the determination of the resonance position has a mean relative uncertainty of 3×10^{-4} .

The magnetic field was calibrated at four magnetic field strengths between 200 and 700 G using the ^{87}Rb $|1, 1\rangle \rightarrow |1, 0\rangle$ RF transition. A residual inhomogeneity of the magnetic field over the trap region and small current noise lead to a relative field width of 3×10^{-4} , restricting the uncertainty of the field calibration to 1×10^{-4} .

Based on the interatomic potential we were able to predict all s-wave Feshbach resonances in the available spin states. All resonances were found less than 0.8 G from the predicted values. The measured resonances are listed in Table I.

The measured resonance positions were then used to refine the molecular potentials further using the method described in Ref. [23]. By slightly altering the dispersive coefficients and the slope of the potential at the inner turning point, an optimal match of the calculated and measured resonance positions was obtained. In this procedure, the experimental observations were weighted with their individual uncertainties. Figure 2 shows the binding energies and the scattering length at the resonances for the ^{87}Rb $|1, 1\rangle$, ^{40}K $|9/2, -5/2\rangle$ state. The calculated resonance positions B_{th} and widths Δ_{th} are listed in Table I. The theoretical widths correspond to the distance between the center of the resonance and the zero crossing of the scattering length. This width corresponds to the usual approximation for the scattering length in the vicinity of a Feshbach resonance $a(B) = a_{\text{BG}}(1 - \frac{\Delta_{\text{th}}}{B - B_{\text{th}}})$ with the background scattering length a_{BG} .

With this procedure, it was possible to improve the consistency of the model significantly. The initial fit to the ten known resonance positions from Ref. [24, 25] gave a mean deviation of 275 mG, 2.75 times larger than the experimental uncertainty of 100 mG. We were able to reduce the mean deviation for our measurement of all 28 resonances to 123 mG, yielding a standard deviation of 1.1 times the experimental uncertainty. Thus, our model

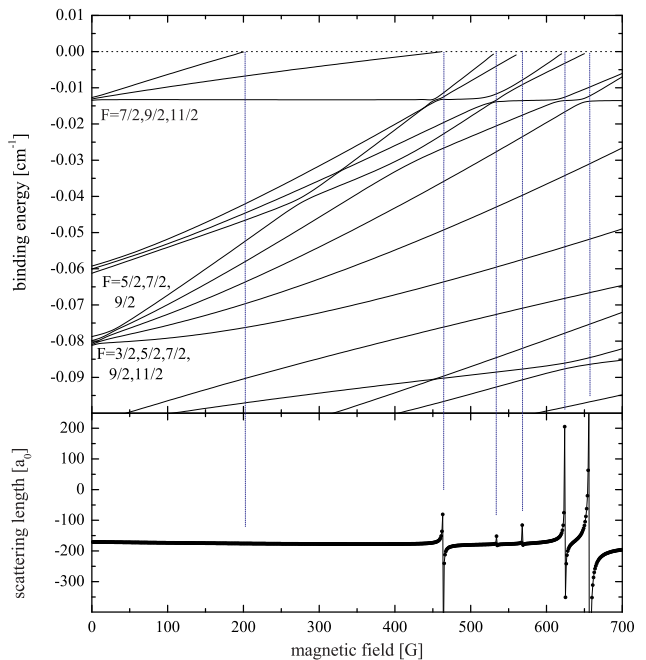


FIG. 2: Simulation of the molecular binding energies as a function of the magnetic field for the ^{87}Rb $|1, 1\rangle$, ^{40}K $|9/2, -5/2\rangle$ state (top). Around the magnetic field positions where the binding energy approaches zero, the heteronuclear scattering length diverges (bottom). The resonances are not fully resolved due to the finite computational step size chosen for the graph. The total angular momentum specified at zero magnetic field is denoted by F .

reproduces all resonance positions within the experimental uncertainty. However, our model does not include the collisional loss processes in the vicinity of a resonance which can slightly shift the resonance positions.

The precise knowledge of the interatomic potential is a key ingredient for many experiments with quantum degenerate heteronuclear mixtures. In particular, our model allows for an accurate calculation of binding energies of the molecular levels, which is an essential ingredient on the way to deeply bound quantum degenerate molecules. The weakly bound levels which are responsible for the Feshbach resonances are listed in Table II. For the lowest singlet and triplet molecular states, we obtain a binding energy of 4180.269 cm^{-1} ($N=0$, hyperfine splitting less than 1 MHz) and 240.024 cm^{-1} ($N=0$, $F=7/2$), respectively.

In combination with a good understanding of the electronically excited molecular potentials, this will allow for the selection of excited states with sufficient Franck-Condon overlap for the transfer of Feshbach molecules to deeply bound molecules. Thus, our results provide a major step on the path towards the production of quantum degenerate ground-state molecules.

Finally, our model allows us to predict Feshbach resonances in mixtures of ^{39}K and ^{87}Rb or ^{41}K and ^{87}Rb .

TABLE II: Binding energies of the involved molecular states in cm^{-1} with respect to the atomic asymptote $f_{\text{Rb}} = 1$, $f_{\text{K}} = 9/2$. The expectation value of the electronic spin is given to quantify the triplet-singlet mixing.

F	$f_{\text{Rb}}/f_{\text{K}}$	spin	binding energy	F	$f_{\text{Rb}}/f_{\text{K}}$	spin	binding energy
$\frac{3}{2}$	$2/\frac{7}{2}$	1	-0.08120	$\frac{9}{2}$	$1/\frac{7}{2}$	0.831	-0.06125
$\frac{5}{2}$	$2/\frac{7}{2}$	0.918	-0.08096	$\frac{7}{2}$	$1/\frac{7}{2}$	0.718	-0.06009
$\frac{7}{2}$	$2/\frac{7}{2}$	0.81	-0.08056	$\frac{5}{2}$	$1/\frac{7}{2}$	0.638	-0.05926
$\frac{9}{2}$	$2/\frac{7}{2}$	0.678	-0.07989	$\frac{3}{2}$	$1/\frac{9}{2}$	0.907	-0.01345
$\frac{11}{2}$	$2/\frac{7}{2}$	0.519	-0.07878	$\frac{1}{2}$	$1/\frac{9}{2}$	0.784	-0.01310
				$\frac{11}{2}$	$1/\frac{9}{2}$	0.628	-0.01269

In Fig. 3, the Feshbach resonances are shown for the stable spin configuration with both species in the $|1, 1\rangle$ state. Both mixtures show broad resonances, which can be used for precise control of the interactions [30]. In particular, the wide resonance at ~ 40 G will allow very precise control of the scattering properties over the full range from $-1500 a_0$ to $1500 a_0$. Both bosonic Potassium-Rubidium mixtures are currently under investigation and will enable an experimental investigation of the predicted resonances. By comparing the resonance positions, it will be possible to test the validity of the Born-Oppenheimer potentials used in this work. The non-zero mass ratio between the electrons and the nuclei leads to corrections to the Born-Oppenheimer potential [31] which result in a phase shift of the scattering states. This shifts the Feshbach resonances slightly with respect to the predictions and an experimental observation will allow for the validation of the mass-scaling techniques with unprecedented precision.

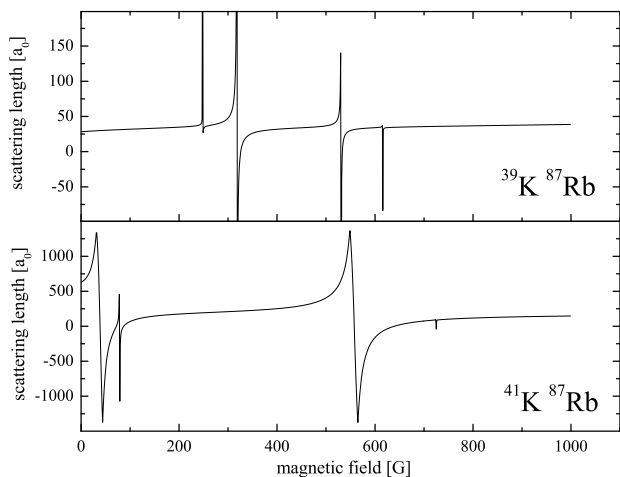


FIG. 3: Interspecies scattering lengths of $^{39}\text{K}^{87}\text{Rb}$ (top) and $^{41}\text{K}^{87}\text{Rb}$ (bottom) as a function of the magnetic field strength.

In conclusion, we have observed 20 previously unknown s-wave Feshbach resonances in a mixture of ^{40}K and ^{87}Rb . Using these observations we have significantly improved the model of the interspecies interaction, which reproduces the experimental data both at small and large internuclear separation. In addition, this potential allows for an accurate calculation of the energy differences between highly excited states and the molecular ground state. This information is of particular relevance for fascinating prospect of forming deeply bound heteronuclear molecules. Finally, the model is used to predict Feshbach resonances in mixtures of ^{87}Rb combined with ^{39}K or ^{41}K . These resonances promise precise control of the bosonic mixtures and also provide a novel system to test the validity of the Born-Oppenheimer approximation.

-
- [1] M. A. Baranov, L. Dobrek, and M. Lewenstein, Phys. Rev. Lett. **92**, 250403 (2004).
 - [2] M. A. Baranov, M. S. Marenko, V. S. Rychkov, and G. V. Shlyapnikov, Phys. Rev. A **66**, 013606 (2002).
 - [3] D. DeMille, Phys. Rev. Lett. **88**, 067901 (2002).
 - [4] A. Micheli, G. K. Brennen, and P. Zoller, Nature Phys. **2**, 341 (2006).
 - [5] M. A. Baranov, K. Osterloh, and M. Lewenstein, Phys. Rev. Lett. **94**, 070404 (2005).
 - [6] J. Stuhler *et al.*, Phys. Rev. Lett. **95**, 150406 (2005).
 - [7] S. Kotochigova, P. S. Julienne, and E. Tiesinga, Phys. Rev. A **68**, 022501 (2003).
 - [8] J. Doyle, B. Friedrich, R. Krems, and F. Masnou-Seeuws, Eur. Phys. J. D **31**, 149 (2004).
 - [9] O. Dulieu, M. Raoult, and E. Tiemann, J. Phys. B **39**, (2006).
 - [10] J. Herbig *et al.*, Science **301**, 1510 (2003).
 - [11] S. Dürr, T. Volz, A. Marte, and G. Rempe, Phys. Rev. Lett. **92**, 020406 (2004).
 - [12] G. Thalhammer *et al.*, Phys. Rev. Lett. **96**, 050402 (2006).
 - [13] S. Jochim *et al.*, Phys. Rev. Lett. **91**, 240402 (2003).
 - [14] C. A. Regal, C. Ticknor, J. L. Bohn, and D. S. Jin, Nature **424**, 47 (2003).
 - [15] S. B. Papp and C. E. Wieman, Phys. Rev. Lett. **97**, 180404 (2006).
 - [16] C. Ospelkaus *et al.*, Phys. Rev. Lett. **97**, 120402 (2006).
 - [17] B. W. Shore, K. Bergmann, and J. Oreg, Z. Phys. D **V23**, 33 (1992).
 - [18] B. Damski *et al.*, Phys. Rev. Lett. **90**, 110401 (2003).
 - [19] S. Kotochigova, E. Tiesinga, and P. S. Julienne, Eur. Phys. J. D **31**, 189 (2004).
 - [20] W. C. Stwalley, Eur. Phys. J. D **31**, 221 (2004).
 - [21] K. Winkler *et al.*, Phys. Rev. Lett. **98**, 043201 (2007).
 - [22] D. Wang *et al.*, Phys. Rev. A **75**, 032511 (2007).
 - [23] A. Pashov *et al.*, in preparation .
 - [24] F. Ferlaino *et al.*, Phys. Rev. A **73**, 040702(R) (2006).
 - [25] F. Ferlaino *et al.*, Phys. Rev. A **74**, 039903(E) (2006).
 - [26] S. Ospelkaus *et al.*, Phys. Rev. Lett. **97**, 120403 (2006).
 - [27] S. Inouye *et al.*, Phys. Rev. Lett. **93**, 183201 (2004).
 - [28] C. Klempt *et al.*, Phys. Rev. A **73**, 13410 (2006).
 - [29] T. Esslinger, I. Bloch, and T. W. Hänsch, Phys. Rev. A

- 58**, R2664 (1998).
- [30] G. Roati *et al.*, cond-mat/0703714 (2007).
- [31] J. K. G. Watson, J. Mol. Spectrosc. **80**, 411 (1980).